Uniaxial Tensile Testing Device for Measuring Mechanical Properties of Biological Tissue with Stress-Relaxation Test under a Confocal Microscope

David Vondrášek[1,2], Daniel Hadraba[1,2], Roman Matějka[2], František Lopot[1], Martin Svoboda[3], Karel Jelen[1]
[1]Faculty of Physical Education and Sport, Charles University, Prague, Czech Republic, E-mail: david.vondrasek@fgu.cas.cz, daniel.hadraba@fgu.cas.cz, flopot@seznam.cz, jelen@ftvs.cuni.cz
[2]Institute of Physiology, Czech Academy, Prague, Czech Republic, E-mail: roman.matejka@fgu.cas.cz
[3]Faculty of Mechanical Engineering, Jan Evangelista Purkyně University in Ústí nad Labem, Pasteurova 1, Ústí nad Labem, Czech Republic, E-mail: martin.svoboda@ujep.cz

Biological soft tissue is a non-linear and viscoelastic material and its mechanical properties can greatly affect quality of life. Many external mechanical factors can alter the tissue, for example the tissue of talipes equinovarus congenitus, also known as clubfoot, which is the most frequent congenital deformity affecting lower extremities with pathological changes of connective tissue. In clubfoot, the presence of disc-like mass of fibrous tissue, resembling intervertebral disc tissue, is described to be between the medial malleolus and the medial side of the navicular bone. The clubfoot tissue is often referred to be stiffer or rigid by clinicians, or it is referred to as contracted and less contracted tissue, however relevant evidence about mechanical properties is missing. Therefore, the description "disc-like" is informing only about relative mechanical properties of clubfoot tissue. We aim to prepare methodical approach to quantify mechanical properties of biological tissue with uniaxial tensile stress-relaxation test, in order to help clinicians and scientist to identify precisely the mechanical properties of normal and pathological tissue and their structural behaviour during mechanical testing. In this study, we test and tune the uniaxial tensile stress-relaxation test on biological tissue with high content of connective tissue such as collagen. The model tissue is porcine pericardium. The tissue has clear collagen fibres aligning parallel to the force applied. Modulus of elasticity measured here is comparable to other studies.

Keywords: uniaxial tensile test, stress-relaxation test, biomechanical models, Maxwell-Wiechert's model, talipes equinovarus congenitus, porcine pericardium, mechanical properties of biological tissues, fibroproliferative diseases

1 Introduction

Biological soft tissues are materials exhibiting viscoelastic and non-linear behaviour to mechanical stimuli [1].Some natural tissues are being used due to this very behaviour in tissue engineering [2] and in engineering [3]. Various types of healthy soft tissues are being studied in regards to their mechanical properties, for example tendons [4],blood vessels [5], muscles [6], brain tissue [7] and eye cornea [8].External mechanical stress can disrupt the soft tissue [9,10], creating abnormalities or forcing the body to start regenerative process [11]. Disruption in the regenerative process of connective tissue can occur [12]. One such disrupted connective tissue is localised at talipes equinovarus congenitus, also known as clubfoot [13,14]. Clubfoot, a severe congenital deformity observed at the area of the foot and lower leg [13,14], is in particular interesting, because it shows signs of fibrosis [12]. Fibrosis is defined as a process of healing damaged tissue, that has gone out of control and the connective tissue is excessively produced at the location of the process [11]. Fibrosis is apparent at medial side of the clubfoot [14], where extracellular matrix is abundant due to fibroproliferative cell activity [15]. Even though the aetiology of the anatomical abnormalities remains unclear, there are suggestions of mechanical causative [12]. It seems, that external forces might have caused the clubfoot deformity [16] with distinct anatomical abnormalities, which keep the foot in apparent supinated position [13].

One important feature of the fibrotic tissue is its increased stiffness compared to other tissue textures [11]. Fibrotic tissue is located on the medial side of the clubfoot, where the tissue is contracted with maximally contracted part being localized between the medial malleolus and the medial side of the navicular bone, while the lateral side of the clubfoot is elongated [14]. Maximally contracted part of the clubfoot, known as 'disc-like tissue', is macroscopically different from surrounding tissue in terms of stiffness, in which it is similar to intervertebral disks [14]. The clubfoot tissue is often referred to be stiffer or rigid by clinicians [17], or it is referred to as contracted and less contracted tissue [18].Almost all of the clubfoot's connective tissue is under mechanical tension [14], however quantitative data about clubfoot's mechanical properties is absent. Increasing diameter of the connective tissue due to proliferation and deposition of extracellular matrix would result in stiffness [19]. However the increase in stiffness would be only relative to the diameter of the tissue, meaning that once normalised, a same amount of tensile stress would be required [20]. On the other hand, if cross-links in the pathological tissue were formed, they could contribute to the stiffness and so mechanical properties of the tissue would change even after normalisation compared with normal state [19]. Therefore, both proper modelling of mechanical behaviour and visualisation are required to uncover properly mechanical properties of an observed tissue.

Looking at stiffness and rigidity of both normal and abnormal soft tissue, we have to always consider its extracellular matrix, to which mechanical properties are tight to [21]. In general, extracellular matrix consists of collagen amongst other proteins [21]. Fibrillary collagen

is in particular interesting due to its non-centrosymmetric structure, which is suitable for label-free second harmonic generation microscopy [22].Second harmonic generation microscopy (SHG) is use to visualize biological tissues, in our case type I and II collagen fibrils [22], without introducing artifacts to the structures by fluorescent staining [23]. Type I collagen fibrils, main component of connective tissue [22], are thick with diameter close to the resolution limits of visible light [24].

Describing the full behaviour of soft tissue requires nonlinear viscoelastic models [1], however linear assumptions can be applied over a narrow band of stress, where equal stress causes equal strains [25]. Extracellular matrix within soft tissue is viscoelastic, therefore its mechanical properties are time/frequency dependent [21]. Time/frequency dependent behaviour of biological tissue can be demonstrated by applying fixed external stress to the tissue and observe a decrease of the initial stress generated within the tissue over time [21]. This is known as stress-relaxation test [21].

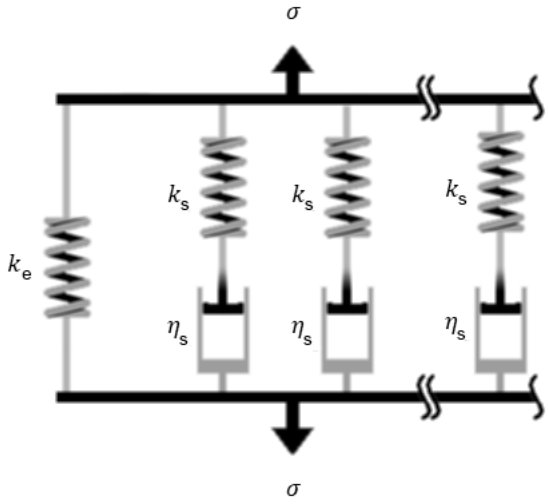

Fig. 1 *Maxwell-Wiechert's model for materials with linear mechanical response to external stress.*

Viscoelastic behaviour of biological tissue can be modelled for example by using Maxwell-Wiechert's model, also known as generalized Maxwell model [26] (Fig. 1). This model is normally used only for linear behaviour of the biological tissue under isothermal conditions [1]. In the model, a spring is connected in parallel with several Maxwell models, which uses springs and dashpot connected in series to describe viscoelastic behaviour [26]. When elastic elements are modelled as springs with constant stiffness, the mechanical response of the elastic component is described by an equation:

$$\sigma_s = k\epsilon \tag{1}$$

where σ represent a stress in the tissue and ϵ displacement or constant strain level, while k is constant, analogous to the Young's modulus E [4,26]. Viscose elements are modelled as dashpots and described by an equation:

$$\sigma_d = \eta\dot{\epsilon} \tag{2}$$

where η is viscosity and $\dot{\epsilon}$ is time derivative of strain (velocity of deformation). The strain of the Maxwell model is equal to the sum of strain $\epsilon_s$of the spring and the strain ϵ_d of the dashpot:

$$\epsilon = \epsilon_s + \epsilon_d \tag{3}$$

while the stress of the Maxwell model is the same for the spring σ_s and for the dashpot σ_d:

$$\sigma = \sigma_s + \sigma_d \tag{4}$$

When the Maxwell model is connected in parallel with an arm containing another spring, the stress of the model is equal to the sum of the stress σ_m in Maxwell model arm with the stress σ_e in parallel spring arm:

$$\sigma = \sigma_m + \sigma_e \tag{5}$$

where σ_e is defined formally with the same relationship as in (1) with its own stiffness (modulus of elasticity). This is an equation for Maxwell-Wiechert's model with only one Maxwell model arm, which has been used in this study. Because both arms of the model are connected in parallel, both of the arms of the model are deformed with the same strain:

$$\epsilon = \epsilon_m + \epsilon_e \tag{6}$$

where ϵ_m is a strain in Maxwell model arm and ϵ_e is a strain in spring arm.

When the described model is used in stress-relaxation test with the relationships described so far, then the decrease of stress is described with equation:

$$\sigma = (\epsilon_0 \,.\, k_e) + (\epsilon_0 \,.\, k_s \,.\, e^{-\frac{k_s}{\eta} \times t}) \tag{7}$$

where ϵ_0 is a strain at time $t = 0$, k_e is modulus of elasticity in the parallel spring arm, k_s is modulus of elasticity in spring within Maxwell model arm, e is Euler's number and t is time. When the time is approaching the infinity (fully relaxed state), the residual stress is equal to the stress in the parallel spring, therefore only to the elastic element of the model. At the time $t = 0$, which is the time when we apply initial stress through deformation ϵ_0, the stress is equal to the sum of parallel and serial stiffness (Fig. 2).

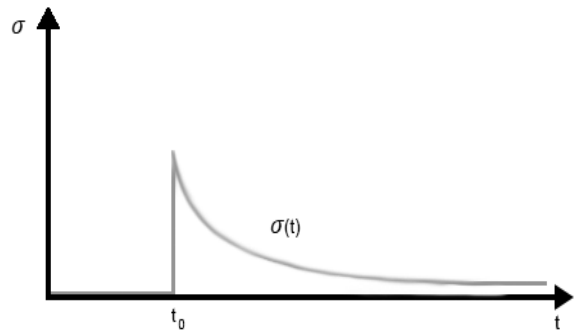

Fig. 2 *Stress-relaxation curve. After a sample-specific time, the sample relaxes.*

The purpose of this study is to create methodical approach to quantify mechanical properties of connective tissue and soft tissue in general using stress-relaxation tensile testing with simultaneous visualization of the tissue using SHG microscopy. We expect that samples of connective tissue will not be showing increased stiffness with greater diameter, rather all the samples will require same amount of tensile stress after normalization to the diameter of the sample. This study is preliminary for testing pathological fibrous tissue of clubfoot.

2 Materials and methods

We used tissue model for uniaxial tensile stress-relaxation test. The tissue model used was porcine pericardium, which was decellularized using sodium dodecyl sulphate (SDS) with concentration of 0.5 %. Remaining SDS was washed out with phosphate-buffered saline (PBS). The tissue should retain its mechanical properties even without cells [27]. Altogether, we used 20 porcine pericardia (one individual), which were cut into rectangles with dimensions of 18.3 mm (± 2.2 mm) x2.5 mm (± 0.4 cm). Two types of groups were created, rectangles with fibres perpendicular to the axis of cutting and rectangles with parallel fibres to the axis of cutting. The height of the samples was measured using reflectance mode of imaging on Leica SPE upright microscope, where we detected reflected light from the surface of rectangles and calculated their height comparing its position to the position of the reflected light from glass surface. The height of the samples was 0.283 mm (± 0.064 mm) and the diameter of the pericardium was calculated. Diameter of perpendicular rectangles was 0.64 mm (± 0.15 mm), while diameter of parallel rectangles was 0.75 mm (± 0.29).

Pericardium rectangles were placed into uniaxial tensile device as shown in Fig. 3. Pericardium rectangles were placed into the jaw grips at 9 mm of starting length and were stretched at the rate of 0.201 mm/s with elongation being 3 % of starting length. Altogether, 25 cycles have been collected, unless tissue rupture has occurred. Between each cycle, we waited for 20 seconds for the tissue to relax, due to its viscosity, which appeared to be sufficient to get resting tension. This approach allowed us to separated response of the sample during constant tension into elastic component and viscose component. We modelled the mechanical response using generalised Maxwell-Wiechert's model with one Maxwell model arm (described above). The uniaxial testing device measured force response of the sample dependent on the stress. The measured force in the tissue was normalised by the diameter of the sample:

$$\sigma(t) = \frac{F(t)}{A_0} \tag{8}$$

where $F(t)$ is the immediate force and A_0 is the cross-sectional area of the pericardium before stress loading the sample. Because the focus of the experiment was the modulus of elasticity, the parameter of the elastic component of the sample, we used the following equation:

$$\sigma = E \tag{9}$$

where E is the Young's modulus of elasticity and ϵ is a deformation of the sample l relative to the previous length l_0:

$$\epsilon = \frac{l}{l_0} \tag{10}$$

Viscose component as a time dependent component is only present as a decrease in the tension within the sample during relaxation until the forces in the sample settle down. Looking at equation (7), at the time $t = 0$, the viscose element is not contributing to the tension of the Maxwell-Wiechert's model and only the spring of the Maxwell model arm with parallel spring are contributing to the tension. After initial deformation was applied, the sample starts to relax (decrease in tension), because the dashpot is now active. When the forces in the sample settle down, then only the elastic component of the parallel spring is contributing to the resting tension. The elastic component is dependent only on the value of initial stress applied, and not on time. We have evaluated Young's modulus of elasticity, in order to compare the elastic mechanical response of the sample to literature. The data to calculate Young's modulus were obtained from charts containing resting tension plotted against elongation of the sample, which was fitted by linear regression.

Uniaxial tensile device used during testing was self-assembled. The base of the device is two carrying heads with stepper motors, which are moving alongside screw-threaded leading poles. Screw-threaded leading poles are connected to jaws carrying jaw grips for sample placement. Motors are moving against each other and final position of the sample remains unchanged relative to the solid construction of the uniaxial tensile device. Unchanged position of the sample allows placing the device under either upright or inverted microscope and observes the changes with sample's structure "on-line". Small dimensions of the device are compatible with the microscope being used in this study, while using air objective HC PL FLUOTAR 10x/0.30 NA with working distance of 11 mm. Mechanical data were collected using LabView software and were processed in Excel and Matlab.

We used ARDUINO to control the motors and to collect the data from sensors with combination of factory drivers of motors. The minimal step of the jaw's positioning is 0.005 mm. The maximum force of the device is 80 N at the rate of the movement ranging from 0.02 to 1.2 mm/s.

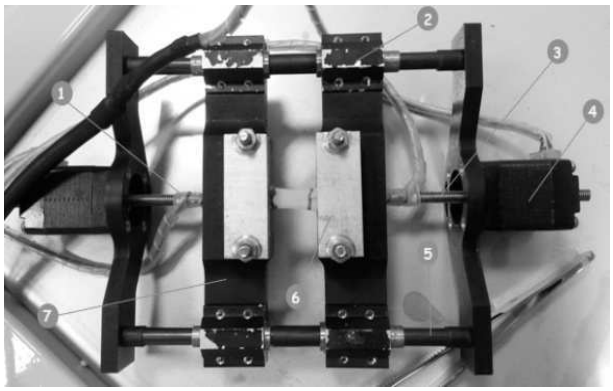

Fig. 3 *Uniaxial tensile device. 1) Force sensor, 2)jaw carrier, 3) screw-threaded leading pole for motors, 4) motor, 5)leading pole, 6) jaw grip, 7) jaws.*

During the relaxing period of the tissue, we collected image data from the samples. Images were collected with Leica SP8 AOBS WLL MP inverted microscope. Multiphoton laser, Chameleon Ultra I (Coherent Inc., CA) was used to generate SHG signal. SHG signal was collected on non-descanned hybrid detectors with superior signal-to-noise ratio. Laser was tuned to 860 nm and emitted light was collected using a bandpass filter 430DF15 for SHG signal and 610/75 for tissue autofluorescence. Image data were processed in ImageJ/Fiji.

3 Results and discussion

Visual data suggest that during stretching of the samples, fibres always align parallel to the force direction (Fig. 4 and Fig. 5). Autofluorescence of the samples was mostly absent. It seems that pericardium tissue exhibits optical anisotropy, when comparing parallel and perpendicular rectangles.

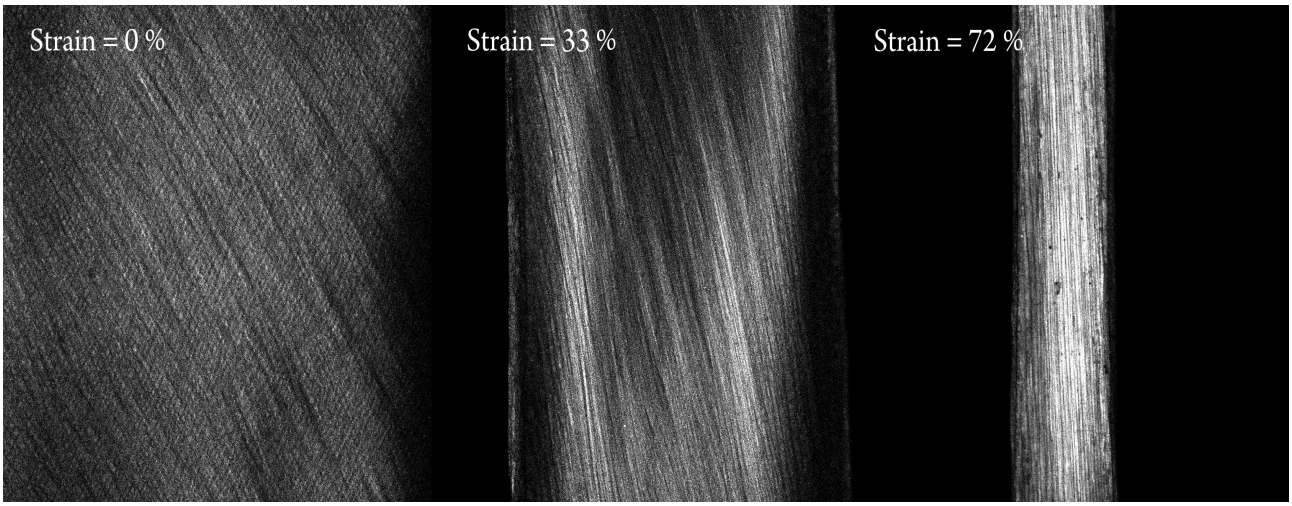

Fig. 4 *Representative pericardium sample, from group of parallel rectangles, three image sequence dependent on the strain applied.*

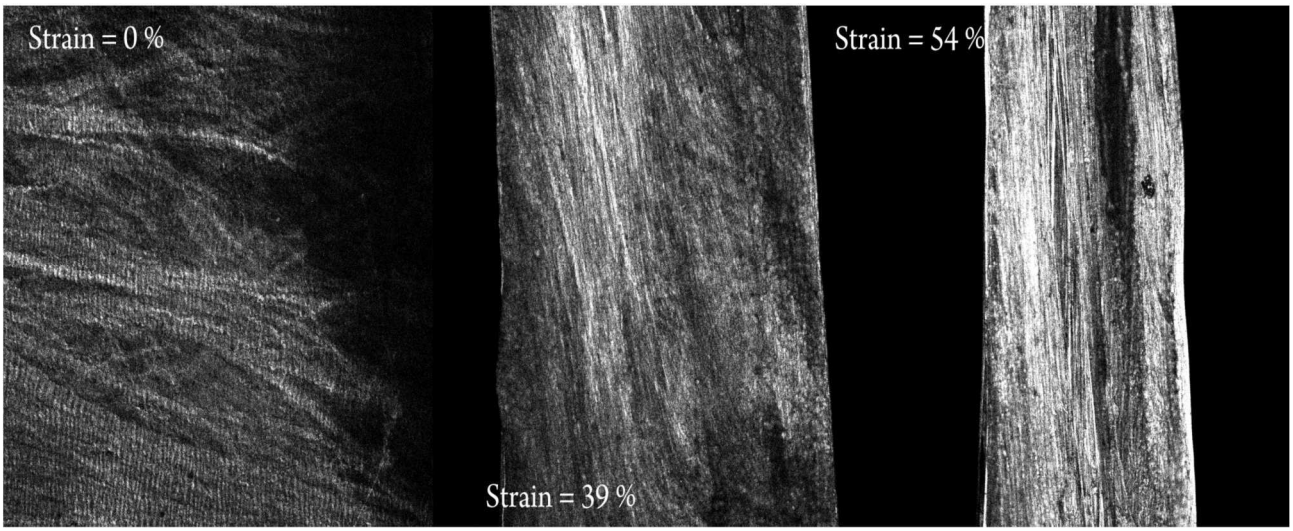

Fig. 5 *Representative pericardium sample, from group of perpendicular rectangles, three image sequence dependent on the strain applied.*

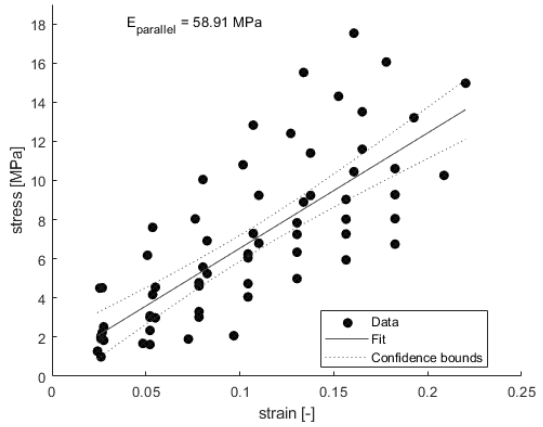

Fig. 6 *Young's modulus of elasticity in pericardium with parallel oriented fibres. Red line is fitting the data.*

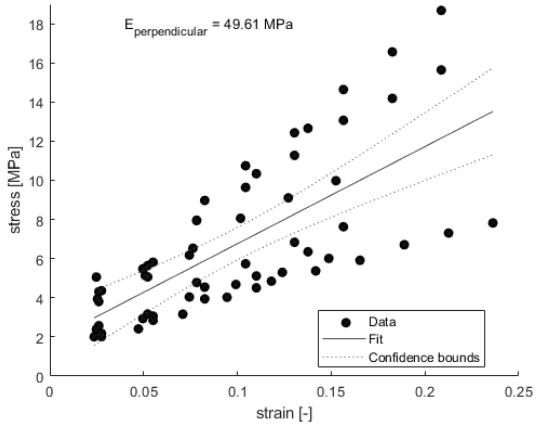

Fig. 7 *Young's modulus of elasticity in pericardium with perpendicular oriented fibres. Red line is fitting the data.*

Porcine pericardium has a modulus of elasticity of 58.91 MPa, when stress is applied in parallel to macroscopic visual orientation of fibres (Fig. 6). When applying stress perpendicular to the orientation, the modulus of elasticity is 49.61 MPa (Fig. 7).Similarity in values of elasticity moduli between two orthogonal directions of pericardium suggest its overall isotropic behaviour, as it was stated in other studies of pericardium's mechanical properties [28], but does not necessarily dispute optical and mechanical anisotropy of the tissue [29]. Our results are corresponding to previously measured moduli of elasticity in bovine pericardium by Sizeland *et al.*, who have measured modulus of elasticity in neonatal (80 MPa) and adult (30 MPa) individuals, with younger individuals having higher modulus of elasticity [30]. It seems that modulus of elasticity is age dependent and it should be considered when combining samples from young and old individuals. Our data also correspond with values found in donkey's pericardium (80 MPa) [31] and other bovine pericardia [32]. Many other studies have measured the modulus of elasticity in various pericardia, however, values are ranging from 10 MPa to 300 MPa [29,33]. Gauvin *el al*. have showed differences between bovine and porcine pericardium [34], suggesting high variability in-between species.

It is important to note another potential source of variability in mechanical properties of biological soft tissue. One of the most influential factors affecting mechanical response of the tissue to external pressure is hydration [35]. For example, mechanical behaviour of pig-arterial elastin changes with hydration in such a way, that modulus of elasticity in dry elastin increases so much that it loses its rubber-like behaviour and behaves like a brittle polymeric glass [36]. Individual collagen fibres behave in a similar way. Grant *et al.* tested individual fibres of collagen from bovine Achilles tendons and observed significant drop in Young's modulus of elasticity, when measured dry and hydrated, from 1.9 ± 0.5 GPa to just 1.2 ± 0.1 MPa, respectively [37]. Furthermore, Andriotis et al. observed shrinking and stiffening of collagen fibres, when dehydrating fibres by controlling osmotic pressure in the measuring solution [35]. Therefore, it is important to improve the uniaxial tensile stress-relaxation testing device solely for upright microscope, so that it would be possible for the user of the device to have the sample in solution and control the osmotic pressure and hydration of the sample.

4 Conclusion

The pericardium sample is clearly isotropic material, which is compliant with the literature. The design of the uniaxial tensile device ensures stable position of the sample relative to the objective of the microscope and so it allows direct visualisation of the changes within the structure during the application of external mechanical stress.

The potential of uniaxial tensile stress-relaxation tests using our device remains to be explored further, as a high variability exists in between individuals and with hydration conditions of the sample. The values measured by the uniaxial tensile device in stress-relaxation are comparable with literature, however further tests of the tensile device are required with various types of biological samples. Using uniaxial tensile testing with other means of testing, such as image acquisition, may resolve uncertainties in mechanical testing and can help enlarge the knowledge of tissue's mechanical properties. Further development of the uniaxial device will focus on keeping the sample hydrated with additional option of controlling the osmotic pressure.

Acknowledgement

We acknowledge support by project PROGRES Q41. Furthermore, we acknowledge the BioImaging Facility, Institute of Physiology, supported by the Czech-BioImaging large RI project (LM2015062 funded by MEYS CR) for their support with obtaining scientific data presented in this paper.

References

[1] HASLACH, H. W. (2005) "Nonlinear Viscoelastic, Thermodynamically Consistent, Models for Biological Soft Tissue," *Biomech. Model. Mechanobiol*., 3(3), pp. 172–189.

[2] BADYLAK, S., FREYTES, D., AND GILBERT, T. (2009) "Extracellular Matrix as a Biological Scaffold Material: Structure and Function," *Acta Biomater*., 5(1), pp. 1–13.

[3] VALÁŠEK, P. (2017). "Tensile Strength of Sisal/Epoxy Composites Prepared by Vacuum Infusion," *Manuf. Technol*., 17, pp. 869–874.

[4] DUENWALD, S. E., VANDERBY, R., AND LAKES, R. S. (2009). "Viscoelastic Relaxation and Recovery of Tendon," *Ann. Biomed. Eng*., 37(6), pp. 1131–1140.

[5] L'HEUREUX, N., PÂQUET, S., LABBÉ, R., GERMAIN, L., AND AUGER, F. A. (1998). "A Completely Biological Tissue-Engineered Human Blood Vessel," *FASEB J.*, 12(1), pp. 47–56.

[6] KJAER, M. (2004). "Role of Extracellular Matrix in Adaptation of Tendon and Skeletal Muscle to Mechanical Loading," *Physiol. Rev*., 84(2), pp. 649–698.

[7] MILLER, K., AND CHINZEI, K. (2002). "Mechanical Properties of Brain Tissue in Tension," *J. Biomech*., 35(4), pp. 483–490.

[8] THOMASY, S. M., KRISHNA RAGHUNATHAN, V., WINKLER, M., REILLY, C. M., SADELI, A. R., RUSSELL, P., JESTER, J. V., AND MURPHY, C. J. (2014). "Elastic Modulus and Collagen Organization of the Rabbit Cornea: Epithelium to Endothelium," *Acta Biomater.*, 10(2), pp. 785–791.

[9] SVOBODA, M., SOUKUP, J., JELEN, K., AND KUBOVÝ, P. (2015). "Effect of Impacts on Human Head," *Manuf. Technol*., 15, pp. 226–231.

[10] BITTNER, V., TUČEK, R., PANSKÁ, Š., SVOBODA, M., AND JELEN, K. (2017). "Using the Fourier Transform in the Analysis of Vibration Load Tests of Heterogeneous Mechanical Systems," *Manuf. Technol*., 17, pp. 836–841.

[11] HINZ, B. (2009). "Tissue Stiffness, Latent TGF-B1 Activation, and Mechanical Signal Transduction: Implications for the Pathogenesis and Treatment of Fibrosis," *Curr. Rheumatol. Rep*., 11(2), pp. 120–126.

[12] SIAPKARA, A., AND DUNCAN, R. (2007). "Congenital Talipes Equinovarus," *Bone Jt. J*., 89(8), pp. 995–1000.

[13] COOKE, S. J., BALAIN, B., KERIN, C. C., AND KIELY, N. T. (2008). "Clubfoot," *Curr. Orthop*., 22(2), pp. 139–149.

[14] OŠT'ÁDAL, M., ECKHARDT, A., HERGET, J., MIKŠÍK, I., DUNGL, P., CHOMIAK, J., FRYDRYCHOVÁ, M., AND BURIAN, M. (2015). "Proteomic Analysis of the Extracellular Matrix in Idiopathic Pes Equinovarus," *Mol. Cell. Biochem*., 401(1–2), pp. 133–139.

[15] SANO, H., UHTHOFF, H. K., JARVIS, J. G., MANSINGH, A., AND WENCKEBACH, G. F. C. (1998). "Pathogenesis of Soft-Tissue Contracture in Club Foot," *J. Bone Jt. Surg*., 80(4), p. 4.

[16] ANAND, A., AND SALA, D. A. (2008). "Clubfoot: Etiology and Treatment," *Indian J. Orthop*., 42(1), pp. 22–28.

[17] RAMPAL, V., CHAMOND, C., BARTHES, X., GLORION, C., SERINGE, R., AND WICART, P. (2013). "Long-Term Results of Treatment of Congenital Idiopathic Clubfoot in 187 Feet: Outcome of the Functional 'French' Method, If Necessary Completed by Soft-Tissue Release," *J. Pediatr. Orthop*., 33(1), pp. 48–54.

[18] POON, R., LI, C., AND ALMAN, B. A. (2009). "Beta-Catenin Mediates Soft Tissue Contracture in Clubfoot," *Clin. Orthop*., 467(5), pp. 1180–1185.

[19] CHRISTIANSEN, D. L., HUANG, E. K., AND SILVER, F. H. (2000). "Assembly of Type I Collagen: Fusion of Fibril Subunits and the Influence of Fibril Diameter on Mechanical Properties," *Matrix Biol*., 19(5), pp. 409–420.

[20] LAKES, R. (1993). "Materials with Structural Hierarchy," Nature [Online]. Available: https://www.nature.com/articles/361511a0. [Accessed: 09-Jul-2018].

[21] PURSLOW, P. P., WESS, T. J., AND HUKINS, D. W. (1998). "Collagen Orientation and Molecular Spacing during Creep and Stress-Relaxation in Soft Connective Tissues.," *J. Exp. Biol*., 201(1), pp. 135–142.

[22] SU, P.-J., CHEN, W.-L., LI, T.-H., CHOU, C.-K., CHEN, T.-H., HO, Y.-Y., HUANG, C.-H., CHANG, S.-J., HUANG, Y.-Y., LEE, H.-S., AND DONG, C.-Y. (2010). "The Discrimination of Type I and Type II Collagen and the Label-Free Imaging of Engineered Cartilage Tissue," *Biomaterials*, 31(36), pp. 9415–9421.

[23] OLIVIER, N., LUENGO-OROZ, M. A., DULOQUIN, L., FAURE, E., SAVY, T., VEILLEUX, I., SOLINAS, X., DEBARRE, D., BOURGINE, P., SANTOS, A., PEYRIERAS, N., AND BEAUREPAIRE, E. (2010). "Cell Lineage Reconstruction of Early Zebrafish Embryos Using Label-Free Nonlinear Microscopy," *Science*, 329(5994), pp. 967–971.

[24] CRAIG, A. S., AND PARRY, D. A. D. (1981). "Growth and Development of Collagen Fibrils in Immature Tissues from Rat and Sheep," *Proc. R. Soc. B Biol. Sci*., 212(1186), pp. 85–92.

[25] DEL POZO, R., TANAKA, E., TANAKA, M., OKAZAKI, M., AND TANNE, K. (2002). "The Regional Difference of Viscoelastic Property of Bovine Temporomandibular Joint Disc in Compressive Stress-Relaxation," *Med. Eng. Phys*., 24(3), pp. 165–171.

[26] ROYLANCE, D., "*ENGINEERING VISCOELASTICITY,*" p. 37.

[27] SCHANER, P. J., MARTIN, N. D., TULENKO, T. N., SHAPIRO, I. M., TAROLA, N. A., LEICHTER, R. F., CARABASI, R. A., AND DIMUZIO, P. J. (2004). "Decellularized Vein as a Potential Scaffold for Vascular Tissue Engineering," *J. Vasc. Surg*., 40(1), pp. 146–153.

[28] LEE, J. M., AND BOUGHNER, D. R. (1981). "Tissue Mechanics of Canine Pericardium in Different Test Environments. Evidence for Time-Dependent Accommodation, Absence of Plasticity, and New Roles for Collagen and Elastin.," *Circ. Res*., 49(2), pp. 533–544.

[29] ZIOUPOS, P., BARBENEL, J. C., AND FISHER, J. (1994). "Anisotropic Elasticity and Strength of Glutaraldehyde Fixed Bovine Pericardium for Use in Pericardial Bioprosthetic Valves," *J. Biomed. Mater. Res*., 28(1), pp. 49–57.

[30] SIZELAND, K. H., WELLS, H. C., HIGGINS, J., CUNANAN, C. M., KIRBY, N., HAWLEY, A., MUDIE, S. T., AND HAVERKAMP, R. G. (2014). "Age Dependent Differences in Collagen Alignment of Glutaraldehyde Fixed Bovine Pericardium," *BioMed Res. Int*., 2014, pp. 1–10.

[31] CHEN, S., XU, L., LIU, Y., LI, Q., WANG, D., WANG, X., AND LIU, T. (2013). "Donkey Pericardium as an Alternative Bioprosthetic Heart Valve Material: DONKEY PERICARDIUM AS BIOPROSTHETIC HEART VALVE," *Artif. Organs*, 37(3), pp. 248–255.

[32] HÜLSMANN, J., GRÜN, K., EL AMOURI, S., BARTH, M., HORNUNG, K., HOLZFUß, C., LICHTENBERG, A., AND AKHYARI, P. (2012). "Transplantation Material Bovine Pericardium: Biomechanical and Immunogenic Characteristics after Decellularization vs. Glutaraldehyde-Fixing: Transplantation Material Bovine Pericardium," *Xenotransplantation*, 19(5), pp. 286–297.

[33] GALVÃO BARROS, J. A., FILIPPIN-MONTEIRO, F. B., DE OLIVEIRA, E. M., CAMPA, A., CATALANI, L. H., DE NOGUEIRA MORAES PITOMBO, R., AND POLAKIEWICZ, B. (2014). "Cytotoxicity of PVPAC-Treated Bovine Pericardium: A Potential Replacement for Glutaraldehyde in Biological Heart Valves: Cytotoxicity of PVPAC-Treated Bovine Pericardium," *J. Biomed. Mater. Res. B Appl. Biomater.*, 102(3), pp. 574–582.

[34] GAUVIN, R., MARINOV, G., MEHRI, Y., KLEIN, J., LI, B., LAROUCHE, D., GUZMAN, R., ZHANG, Z., GERMAIN, L., AND GUIDOIN, R. (2013). "A Comparative Study of Bovine and Porcine Pericardium to Highlight Their Potential Advantages to Manufacture Percutaneous Cardiovascular Implants," *J. Biomater. Appl.*, 28(4), pp. 552–565.

[35] ANDRIOTIS, O. G., DESISSAIRE, S., AND THURNER, P. J. (2018). "Collagen Fibrils: Nature's Highly Tunable Nonlinear Springs," *ACS Nano*, 12(4), pp. 3671–3680.

[36] GOSLINE, J., LILLIE, M., CARRINGTON, E., GUERETTE, P., ORTLEPP, C., AND SAVAGE, K. (2002). "Elastic Proteins: Biological Roles and Mechanical Properties.," *Philos. Trans. R. Soc. B Biol. Sci.*, 357(1418), pp. 121–132.

[37] GRANT, C. A., BROCKWELL, D. J., RADFORD, S. E., AND THOMSON, N. H. (2008). "Effects of Hydration on the Mechanical Response of Individual Collagen Fibrils," *Appl. Phys. Lett.*, 92(23), p. 233902.

10.21062/ujep/192.2018/a/1213-2489/MT/18/5/866